Electronic Structures of Halogenated Ruthenium Porphyrins. Crystal Structure of $RuTFPPCl_8(CO)H_2O$ ($TFPPCl_8$ = Octa-β-chlorotetrakis(pentafluorophenyl)porphyrin)

Eva R. Birnbaum, William P. Schaefer, Jay A. Labinger, John E. Bercaw, and Harry B. Gray*

Arthur Amos Noyes Laboratory, California Institute of Technology, Pasadena, California 91125

Received February 17, 1994[⊗]

Ruthenium(II) octa-β-halotetrakis(pentafluorophenyl)porphyrins ($RuTFPPX_8(CO)$, $RuTFPPCl_8(py)_2$; X = Cl, Br) have been synthesized, and the crystal structure of $RuTFPPCl_8(CO)H_2O$ has been determined: $C_{57}H_{28}Cl_8F_{20}N_4O_5Ru$, monoclinic, space group $P2_1/c$, a = 14.364(3) Å, b = 16.012(4) Å, c = 26.679(8) Å, β = 90.29(2)°, V = 6136(3) Å^3, Z = 4, R_w = 0.028 on F^2 for 8005 reflections, R_F = 0.067 for 5378 reflections with $F_o^2 > 3\sigma(F_o^2)$; the porphyrin is highly distorted, with 0.68 and 1.11 Å average displacements of the β-chlorine atoms from the mean porphyrin plane. The reduction potentials of $RuTFPPX_8$ complexes are much more positive (> 0.5 V) than those of unhalogenated analogues, owing to the influence of the electron-withdrawing X atoms. The relatively high energies of the Soret bands in the $RuTFPPX_8$ electronic spectra are consistent with an electronic structural model involving Ru^{II} back-bonding to the porphyrin eπ^* orbitals.

Introduction

We are investigating the structures and properties of metal complexes containing octa-β-halotetrakis(pentafluorophenyl)-porphyrins ($TFPPX_8$; X = Cl, Br) and related halogenated ligands.[1−17] Iron derivatives of the saddle-shaped $TFPPX_8$ ligand are of special interest, owing to their ability to catalyze the oxygenation of alkanes at relatively low temperatures and pressures.[1−3,17] The $Fe^{III/II}$ reduction potentials are unusually high in $FeTFPPX_8^+$ complexes, and both Fe^{III} and Fe^{II} are believed to play an active role in the catalytic reactions.[17,18]

We have extended our work on halogenated porphyrins to include several Ru^{II} derivatives. Here we report the crystal structure of $RuTFPPCl_8(CO)H_2O$ and the electrochemical properties and electronic spectra of $RuTFPPX_n(CO)$ and $RuTFPPCl_n(py)_2$ (n = 6−8) complexes.

Results and Discussion

Insertion of Ru from $Ru_3(CO)_{12}$ into H_2TFPPX_8 in perfluorobenzene yields a bright red (X = Cl) or green (X = Br) $RuTFPPX_8(CO)$ compound. In perprotiobenzene, the extended time at reflux necessary to insert the ruthenium atom results in partial porphyrin dehalogenation and decomposition. In these reactions, ruthenium also inserts into the partially chlorinated derivatives $H_2TFPPCl_7$ and $H_2TFPPCl_6$ to form $RuTFPPCl_7(CO)$ and $RuTFPPCl_6(CO)$, which can be isolated by sequential column and high performance liquid chromatography.

A single band attributable to CO stretching (1990 cm^{-1}, Cl_8; 1973 cm^{-1}, Br_8) is observed in the IR spectrum of $RuTFPPX_8(CO)$.[19] Identification of the other axial ligand is problematic; this ligand is labile in Ru(CO) porphyrins due to the strong trans effect of the CO.[20] Overlapping sets of C_6F_5 resonances in the ^{19}F-NMR spectrum are evidence that the position trans to the carbonyl can be occupied by one of several different ligands. Each pattern has five unique fluorine resonances for the pentafluorophenyl rings, suggesting unsymmetric coordination around the metal center.[14] Photolysis of $RuTFPPCl_8(CO)$ in pyridine results in the formation of $RuTFPPCl_8(py)_2$. After photolysis, a single symmetrically coordinated species is observed by ^{19}F-NMR spectroscopy, indicating that the multiple signals in the spectrum of the carbonyl complex are due to variations in trans ligation and not dehalogenation of the porphyrin ring.

Recrystallization of $RuTFPPCl_8(CO)$ in air from ethyl acetate and hexane gave $RuTFPPCl_8(CO)H_2O$ (Figure 1). An ethyl acetate is hydrogen bonded to the water ligand (O···O = 2.668 Å), and the stability provided by this hydrogen bond network may explain why no crystals were obtained with other solvents.

† Contribution No. 8931.

[⊗] Abstract published in *Advance ACS Abstracts,* February 15, 1995.

(1) Ellis, P. E., Jr.; Lyons, J. E. *Coord. Chem. Rev.* **1990**, *105*, 181−193.
(2) Ellis, P. E., Jr.; Lyons, J. E. *Catal. Lett.* **1989**, *3*, 389−398.
(3) Lyons, J. E.; Ellis, P. E., Jr. *Catal. Lett.* **1991**, *8*, 45−52.
(4) Traylor, T. G.; Tsuchiya, S. *Inorg. Chem.* **1987**, *26*, 1338−1339.
(5) Traylor, T. G.; Hill, K. W.; Fann, W.; Tsuchiya, S.; Dunlap, B. E. *J. Am. Chem. Soc.* **1992**, *114*, 1308−1312.
(6) Bartoli, J. F.; Brigaud, O.; Battioni, P.; Mansuy, D. *J. Chem. Soc., Chem. Commun.* **1991**, 440−442.
(7) Mandon, D.; Ochsenbein, P.; Fischer, J.; Weiss, R.; Jayaraj, K.; Austin, R. N.; Gold, A.; White, P. S.; Brigaud, O.; Battioni, P.; Mansuy, D. *Inorg. Chem.* **1992**, *31*, 2044−2049.
(8) Hoffmann, P.; Robert, A.; Meunier, B. *Bull. Chem. Soc. Fr.* **1992**, *129*, 85−97.
(9) Rocha Gonsalves, A. M. d.; Johnstone, R. A. W.; Pereira, M. M.; Shaw, J.; Sobral, A. J. F. d. N. *Tetrahedron Lett.* **1991**, *32*, 1355−1358.
(10) Wijesekera, T.; Matsumoto, A.; Dolphin, D.; Lexa, D. *Angew. Chem.* **1990**, *29*, 1028−1030.
(11) Marsh, R. E.; Schaefer, W. P.; Hodge, J. A.; Hughes, M. E.; Gray, H. B.; Lyons, J. E.; Ellis, P. E., Jr. *Acta Crystallogr.* **1993**, *C49*, 1339−1342.
(12) Schaefer, W. P.; Hodge, J. A.; Hughes, M. E.; Gray, H. B.; Lyons, J. E.; Ellis, P. E., Jr.; Wagner, R. W. *Acta Crystallogr.* **1993**, *C49*, 1342−1345.
(13) Henling, L. M.; Schaefer, W. P.; Hodge, J. A.; Hughes, M. E.; Gray, H. B.; Lyons, J. E.; Ellis, P. E., Jr. *Acta Crystallogr.* **1993**, *C49*, 1745−1747.
(14) Birnbaum, E. R.; Hodge, J. A.; Schaefer, W. P.; Marsh, R. E.; Henling, L. M.; Labinger, J. A.; Bercaw, J. E.; Gray, H. B. *Inorg. Chem. submitted.*
(15) Hodge, J. A.; Hill, M. G.; Gray, H. B. *Inorg. Chem.* **1995**, *34*, 809−812.
(16) Takeuchi, T.; Gray, H. B.; Goddard, W. A., III. *J. Am. Chem. Soc.* **1994**, *116*, 9730−9732.
(17) Grinstaff, M. W.; Hill, M. G.; Labinger, J. A.; Gray, H. B. *Science* **1994**, *264*, 1311−1313.
(18) Labinger, J. A. *Catal. Lett.* **1994**, *26*, 95−99.
(19) For reference, the CO stretch in the IR spectrum of RuTPP(CO) is at 1945 cm^{-1}: Chow, B. C.; Cohen, I. A. *Bioinorg. Chem.* **1971**, *1*, 57. Since the probable trans ligands (water, ethanol, acetone) are all O atom donors, we would not expect any splitting of ν_{CO}.
(20) Buchler, J. W.; Kokisch, W.; Smith, P. D. *Struct. Bonding* **1978**, *34*, 79−134.

0020-1669/95/1334-1751$09.00/0

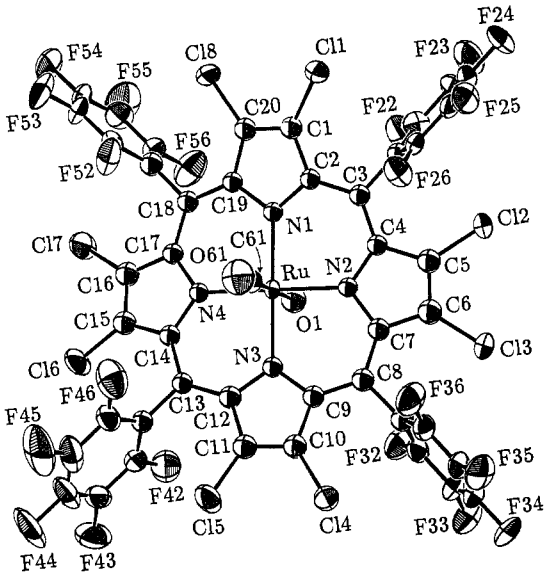

Figure 1. ORTEP diagram of $RuTFPPPCl_8(CO)H_2O$ with 50% probability ellipsoids showing the numbering system used. Atoms C21, C31, C41, and C51 (not numbered) are bonded to C3, C8, C13, and C18, respectively; carbon atoms in the pentafluorophenyl groups have the same numbers as the attached fluorine atoms.

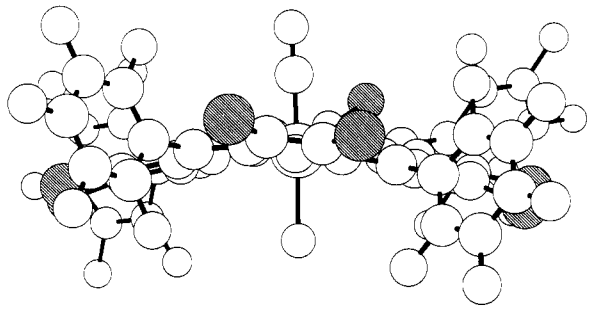

Figure 2. Edge-on view of a Chem 3D drawing of $RuTFPPPCl_8(CO)H_2O$ using crystal structure coordinates. The ruffle in the porphyrin ring is apparent in the different displacements of the chlorine atoms (striped) from the mean plane.

Trans coordination of CO and H_2O to Ru is unusual but is precedented in $RuOEP(CO)H_2O$ and the non-porphyrin compound *trans*-$RuCl_2(PEt_3)_2(CO)H_2O$.[21,22] The $RuTFPPPCl_8$ unit exhibits both the saddle and ruffle distortions common to perhalogenated and other highly substituted porphyrins.[7,11-13,23-25] The saddle distortion is not as severe as in other octachloroporphyrins; the pyrrole carbons are only 0.48 Å from the mean plane compared to 0.625 Å (or 0.74 Å) for $H_2TFPPPCl_8$ (or $ZnTFPPPCl_8$).[14] The ruffle distortion, however, is even more pronounced, with C_{meso} displaced almost twice as far in $RuTFPPPCl_8(CO)H_2O$ as in $ZnTFPPPCl_8$. A side-on view of the porphyrin (Figure 2) reveals a distinct twist in the molecule; within each pyrrole, the two chlorine atoms vary in perpendicular displacements from the mean plane by 0.43 Å. Bond lengths and angles are very similar for all three $TFPPPCl_8$ species.

The Ru−C bond is slightly longer in $RuTFPPPCl_8(CO)H_2O$ (Table 2) than in $RuOEP(CO)H_2O$ (1.785 Å)[21] or $RuTPP(CO)$-EtOH (1.77 Å),[26] consistent with the relatively high value of ν_{CO}.[19] The Ru−C−O bond is nearly linear in the three porphyrins, at 178.9, 178.5, and 175.8°, respectively. The Ru−O bond length (2.172 Å) is shorter for the perhalogenated

Table 1. X-ray Parameters

formula	$C_{57}H_{28}Cl_8F_{20}N_4O_5Ru$
molecular weight	1613.53
color	dark red
shape	rectangular tablet
crystal system	monoclinic
space group	$P2_1/c$
a, Å	14.364(3)
b, Å	16.012(4)
c, Å	26.679(8)
β, deg	90.29(2)
V, Å^3	6136(3)
Z	4
$D_{x,\ g\ cm^{-3}}$	1.75
radiation	MoKα
wavelength, Å	0.710 73
μ, cm^{-1}	7.11
temperature, K	295
crystal size, mm	0.16 × 0.29 × 0.44
diffractometer	Enraf-Nonius CAD-4
collection method	ω scans
θ range, deg	1−22.5
$h_{min/max}$	−15/+15
$k_{min/max}$	−17/+17
$l_{min/max}$	0/28
reflections measured	16 813
independent reflections	8006
reflections used	8005
R_{int}	0.043
$R(F)$	0.089
$R_w(F^2)$	0.028
$(\Delta/\sigma)_{max}$	0.00 (for porphyrin)
goodness of fit	2.72

Table 2. Selected Average Bond Lengths (Å) for $RuTFPPPCl_8(CO)H_2O$

$N-C_\alpha$	1.378	Ru−C	1.828
$C_\alpha-C_\beta$	1.448	Ru−O	2.172
$C_\beta-C_\beta$	1.339	C−O	1.134
$C_\alpha-C_m$	1.399	Ru−N	2.059

Table 3. Selected Average Angles (deg) for $RuTFPPPCl_8(CO)H_2O$

N−Ru−N	175.5	$C_\alpha-C_\beta-C_\beta$	108.0
C−Ru−O	177.6	$C_\alpha-C_m-C_\alpha$	126.0
$N-C_\alpha-C_m$	125.1	$C_m-C_\alpha-C_\beta$, dihedral (C_6F_5 groups)	127.0
$N-C_\alpha-C_\beta$	107.8		

Table 4. Average Deviations (Å) of Atoms from the Least-Squares Plane

N	0.06	Cl_{odd}	1.11
C_m	0.20	Cl_{even}	0.68
C_β	0.48	Ru	0.11 (towards CO)

Table 5. Electrochemistry of Halogenated Ruthenium Porphyrins.[a]

porphyrin	$E^{\circ\prime}_{+/0}$	$E^{\circ\prime}_{0/-}$
$RuTFPPPCl_8(CO)$	1.71	−0.64
$RuTFPPPCl_7(CO)$	1.69	−0.69
$RuTFPPPCl_6(CO)$	1.64	−0.76
$H_2TFPPPCl_8$	1.66[b]	−0.32
$RuTFPPPBr_8(CO)$	1.63	−0.84
$H_2TFPPPBr_8$	1.56[b]	−0.31
$RuTFPPPCl_8(py)_2$	1.08	−0.94
$RuTFPPPCl_7(py)_2$	1.04	−0.98
$RuTFPPPCl_6(py)_2$	0.89	−1.12

[a] Potentials in CH_2Cl_2 solution at room temperature (V vs AgCl/Ag, 0.1 M $(TBA)PF_6$). [b] E_{pa}.

(21) Kadish, K. M.; Hu, Y.; Mu, X. H. *J. Heterocycl. Chem.* **1991**, *28*, 1821−1824.
(22) Sun, Y.; Taylor, N. J.; Carty, A. J. *Inorg. Chem.* **1993**, *32*, 4457−4459.
(23) Ochsenbein, P.; Ayougou, K.; Mondon, D.; Fischer, J.; Weiss, R.; Austin, R. N.; Jayaraj, K.; Gold, A.; Terner, J.; Fajer, J. *Angew. Chem.* **1994**, *33*, 348−350.
(24) Bhyrappa, P.; Krishnan, V. *Inorg. Chem.* **1991**, *30*, 239−245.
(25) Barkigia, K. M.; Berber, M. D.; Fajer, J.; Medforth, C. J.; Renner, M. W.; Smith, K. M. *J. Am. Chem. Soc.* **1990**, *112*, 8851−8857.
(26) Bonnet, J. J.; Eaton, S. S.; Eaton, G. R.; Holm, R. H.; Ibers, J. A. *J. Am. Chem. Soc.* **1973**, *95*, 2141−2149.

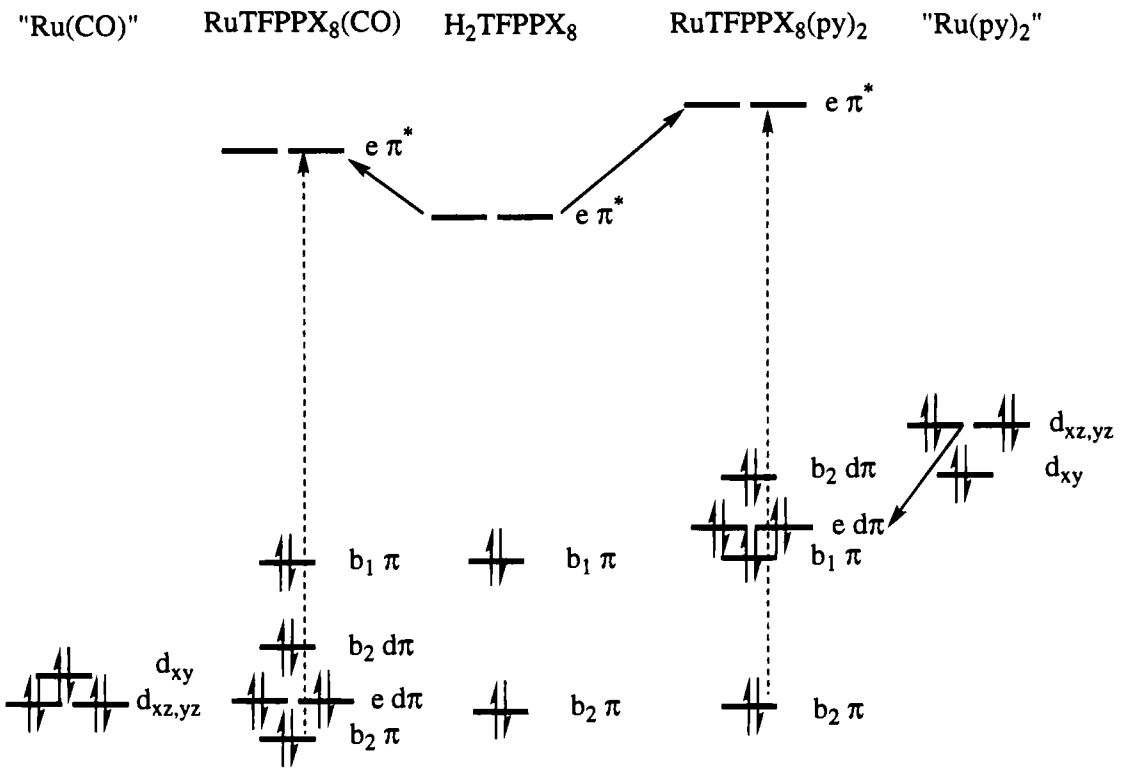

Figure 3. Molecular orbital diagram of the Gouterman orbitals for H_2TFPPX_8 modified by inclusion of interactions with the dπ orbitals of carbonyl and bis(pyridine)ruthenium fragments (D_{2d} labels). Extensive π-back-bonding to the carbonyl ligand strongly stabilizes the d_{xz}, d_{yz} orbitals (and, to a lesser extent, the d_{xy} orbital, owing to the reduction in electron density at the Ru center), resulting in a ligand-based HOMO for $RuTFPPX_8(CO)$. Weaker π-back-bonding in the $Ru(py)_2$ fragment leaves the dπ orbitals at higher energies, consistent with stronger d_{xz}, $d_{yz} \rightarrow \pi^*$ ($TFPPX_8$) interactions and a Ru-based HOMO in $RuTFPPX_8(py)_2$. The Soret transition is shown with a dotted line.

porphyrin than in $RuOEP(CO)H_2O$ (2.253 Å) and closer to the distance found for *trans*-$RuCl_2(PEt_3)_2(CO)H_2O$ (2.189 Å).[21,22] Interestingly, although the Ru–N bond lengths in $RuTFPPCl_8(CO)H_2O$ and RuTPP(CO)EtOH are the same (~2.05 Å), the TPP derivative is planar, whereas the metal in the halogenated derivative is 0.11 Å out of the mean plane toward the carbonyl ligand. The distorted structure apparently decreases the core size and may explain why ruthenium insertion is so difficult for this porphyrin.

The reduction potentials set out in Table 5 are in agreement with other electrochemical data[10,15,23,24,27,28] showing that electron-withdrawing groups at the β positions stabilize both the highest occupied and lowest unoccupied molecular orbitals (HOMOs and LUMOs) of tetraphenylporphyrins. The $RuTFPPX_8(CO)$ complexes, for example, are harder to oxidize and easier to reduce than RuTPP(CO).[29] Notably, the $RuTFPPX_8(CO)^{+/0}$ potentials are within 0.07 V of those of the unmetalated H_2TFPPX_8 molecules. Oxidation of $RuTFPPCl_8(py)_2$ occurs 0.63 V lower than $RuTFPPCl_8(CO)$, suggesting that the HOMO is a dπ level in the pyridine derivative (as established for $RuTPP(py)_2$).[30]

Both calculations[16,31] and electrochemical measurements[15,23–25,32,33] indicate that the S_4 (saddle) distortions destabilize the HOMOs more than the LUMOs of β-substituted porphyrins. This sterically induced contraction of the HOMO–LUMO gap is surprisingly small for $RuTFPPCl_8(CO)$ (0.11 V relative to RuTPP(CO)[29] from the values of the +/0 and 0/− potentials). Enhanced back-bonding from Ru^{II} to $TFPPCl_8$ is the likely explanation of this finding, as discussed below.

The electronic properties of perhalogenated Ru^{II} porphyrins can be interpreted in terms of a Gouterman four-orbital model[16,34] modified by the inclusion of the Ru dπ orbitals (Figure 3).[35] Increased back-bonding in the $TFPPX_8$ complexes promotes mixing of $\pi \rightarrow e\pi^*$ and $Ru^{II} \rightarrow e\pi^*$ excited states, with the result that the Soret (mainly $\pi \rightarrow e\pi^*$) transition falls at higher energies than would be predicted by a simple one-electron (HOMO–LUMO) model.[20,36,37] The Soret band of $RuTFPPCl_8(CO)$ (418 nm) is substantially blue-shifted from that of $H_2TFPPCl_8$ (440 nm). Nevertheless, the magnitude of the shift, ~1300 cm^{-1}, is surprisingly high; it indicates that the electronic coupling of Ru^{II} to the porphyrin is unusually strong.[38]

(27) Binstead, R. A.; Crossley, M. J.; Hush, N. S. *Inorg. Chem.* **1991**, *30*, 1259–1264.
(28) Callot, H. J. *Bull. Chem. Soc. Fr.* **1974**, *7*, 1492–1496.
(29) The potentials of RuTPP(CO) are 0.87 (+/0) and −1.59 (0/−) V vs SCE (CH_2Cl_2, 0.1 M TBAP): Mu, X. H.; Kadish, K. M. *Langmuir* **1990**, *6*, 51–56.
(30) The +/0 potential of $RuTPP(py)_2$ is 0.21 V vs SSCE (CH_2Cl_2, 0.1 M TBAH): Brown, G. M.; Hopf, F. R.; Ferguson, J. A.; Meyer, T. J.; Whitten, D. G. *J. Am. Chem. Soc.* **1973**, *95*, 5939–5942.
(31) Barkigia, K. M.; Chantranupong, L.; Smith, K. M.; Fajer, J. *J. Am. Chem. Soc.* **1988**, *110*, 7566–7567.
(32) Giraudeau, A.; Callot, J. H.; Gross, M. *Inorg. Chem.* **1979**, *18*, 201–206.
(33) Senge, M. O.; Medforth, C. J.; Sparks, L. D.; Shelnutt, J. A.; Smith, K. M. *Inorg. Chem.* **1993**, *32*, 1716–1723.
(34) Gouterman, M. *J. Mol. Spectrosc.* **1961**, *6*, 138–163.
(35) Since pyridine is a much weaker π acceptor than CO, we would expect Ru^{II} to back-bond more strongly to $TFPPCl_8$ in the bis(pyridine) than in the carbonyl derivative. For discussions of M^{II} (M = Fe, Ru, Os) back-bonding to CO and py in porphyrin complexes, see: Gentemann, S.; Albaneze, J.; Garcia-Ferrer, R.; Knapp, S.; Potenza, J. A.; Schugar, H. J.; Holten, D. *J. Am. Chem. Soc.* **1994**, *116*, 281–289. Kim, D.; Su, Y. O.; Spiro, T. G. *Inorg. Chem.* **1986**, *25*, 3993–3997. Schick, G. A.; Bocian, D. F. *J. Am. Chem. Soc.* **1984**, *106*, 1682–1694.
(36) Gouterman, M. In *The Porphyrins*; Dolphin, D., Ed.; Academic Press, Inc.: New York, 1978; Vol. III; pp 1–156.
(37) Antipas, A.; Buchler, J. W.; Gouterman, M.; Smith, P. D. *J. Am. Chem. Soc.* **1978**, *100*, 3015–3024.
(38) IR data also indicate that halogenated porphyrins are π acceptors: the peak attributable to the CO stretch decreases according to $RuTFPPCl_8(CO)$ (1990) > $RuTFPPCl_7(CO)$ (1987) > $RuTFPPCl_6(CO)$ (1984) > $RuTFPPBr_8(CO)$ (1973 cm^{-1}).

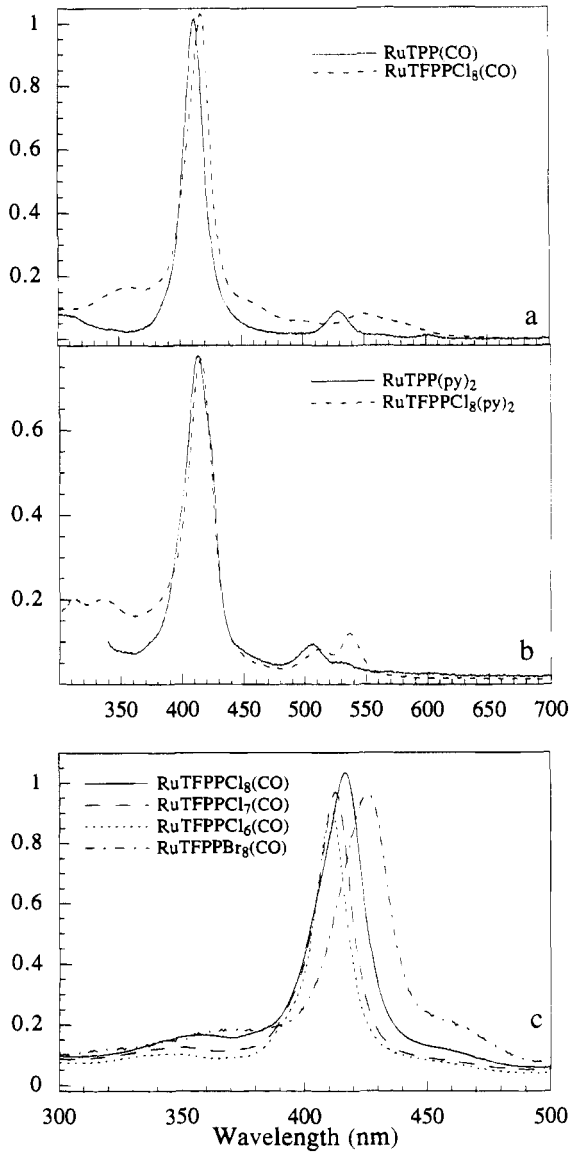

Figure 4. Electronic absorption spectra in CH_2Cl_2 solution at room temperature: (a) RuTPP(CO) and $RuTFPPCl_8(CO)$; (b) $RuTPP(py)_2$ (in pyridine) and $RuTFPPCl_8(py)_2$; and (c) $RuTFPPX_8(CO)$, $RuTFPPCl_7$-(CO), and $RuTFPPCl_6(CO)$. The vertical axis is absorbance.

The offsetting effect of extensive back-bonding in the distorted porphyrins is the reason that the Soret bands for both $RuTFPPCl_8$-(CO) and $RuTFPPCl_8(py)_2$ (416 nm) are only slightly red-shifted from those of RuTPP(CO) (412 nm) and $RuTPP(py)_2$ (413 nm) (Figure 4).

The distortion-induced contraction of the HOMO−LUMO gap[16,23,24,31−33] is evidenced by a decrease of the Soret transition energy according to $RuTFPPCl_6(CO)$ (410) > $RuTFPPCl_7(CO)$ (413.5) > $RuTFPPCl_8(CO)$ (418 nm) (Figure 4c). The Soret band of $RuTFPPBr_8(CO)$ is further red-shifted to 424 nm; as predicted,[16] the larger halogen atoms generate a greater distortion of the porphyrin, thereby producing a smaller HOMO−LUMO gap. Porphyrin saddling also is responsible for the red shifts of the Q(0,1) bands of $RuTFPPX_8$ complexes from those of the corresponding TPP derivatives (Figure 4a,b).

Relatively weak bands at 670 ($\epsilon \approx 800$) and 792 nm ($\epsilon \approx 300\ M^{-1}\ cm^{-1}$) are observed in the spectrum of $RuTFPPCl_8$-$(py)_2$ (not shown in Figure 4). Low-lying $Ru^{II} \rightarrow \pi^*$ ($TFPPCl_8$) transitions are expected, since the electrochemical data show that both Ru^{II} oxidation and $TFPPCl_8$ reduction are accessible. Extensive back-bonding to $e\pi^*$ ($TFPPCl_8$) orbitals would stabilize d_{xz}, d_{yz} relative to d_{xy} (Figure 3); it is likely, then, that a d_{xy} electron is involved in both electrochemical and the 792-nm spectroscopic oxidation of Ru^{II} to Ru^{III}. No bands above 650 nm were observed in the spectrum of $RuTFPPCl_8(CO)$, consistent with the absence of any Ru^{II} oxidations in the electrochemical experiments.

Experimental Section

Materials. Zinc(II) tetrakis(pentafluorophenyl)porphyrin (Zn-TFPP) was used as received from Porphyrin Products. Omnisol grade methanol, acetone, dichloromethane, benzene, pyridine, and hexane were from EM Science. *N*-Chlorosuccinimide, RuTPP(CO), and $Ru_3(CO)_{12}$ were from Aldrich. $RuTPP(py)_2$ was prepared by a literature method.[39]

$RuTFPPCl_8(CO)$. The preparation of $RuTFPPCl_8(CO)$ was based on the methods of Tsutsui[40] and Chow.[41] $H_2TFPPCl_8$[14] (300 mg) reacted with $Ru_3(CO)_{12}$ (48 h, refluxing benzene) to form $RuTFPPCl_8(CO)$. $RuTFPPCl_7(CO)$ and $RuTFPPCl_6(CO)$ also were isolated from the reaction mixture. $RuTFPPCl_n(CO)$ ($n = 6-8$) complexes were purified by HPLC, and the identity of each fraction was confirmed by mass spectroscopy. The parent peak in each mass spectrum appears at the mass for $RuTFPPCl_n$ ($n = 6-8$), with a smaller peak appearing at the mass for the monocarbonyl complex. Parent peaks appeared at $m/z = 1351.2$ ($RuTFPPCl_8$), 1315.8 ($RuTFPPCl_7$), and 1280.1 ($RuTFPPCl_6$). $RuTFPPBr_8(CO)$ (mass spectrum; $m/z = 1703$) was synthesized from $Ru_3(CO)_{12}$ and $H_2TFPPBr_8$ (50 h, refluxing benzene). UV−vis for $RuTFPPCl_8(CO)$ (CH_2Cl_2), λ ($\epsilon/10^4$): 348, 417 (50), 540 (1.3) nm.

$RuTFPPCl_8(py)_2$. Photolysis of the carbonyl was accomplished by modification of Chow's methods.[41] Pyridine solutions of $RuTFPPCl_n(CO)$ exposed to a 1000-W mercury lamp for several hours lose a carbonyl ligand to form $RuTF$-$PPCl_n(py)_2$. Loss of the carbonyl was confirmed by the disappearance of the CO stretch (IR, CCl_4 solution) and by ^{19}F-NMR spectroscopy ($CDCl_3$ solution): $\delta(RuTFPPCl_8(py)_2) = -138.7$ (2F, q, ortho), −152.3 (1F, t, para), −163.2 (2F, m, meta). UV−vis (CH_2Cl_2) λ: 415, 510, 536 nm. ^{19}F-NMR: −138.7 (2F, q, ortho), −152.3 (1F, t, para), −163.2 ppm (2F, m, meta).

Methods. Infrared spectra were recorded as solutions in carbon tetrachloride or benzene on a Perkin-Elmer Model 1600 FT-IR spectrophotometer. Electronic absorption spectra were recorded on an Olis-modified Cary-14 spectrophotometer. Separation of the ruthenium porphyrins was accomplished with a Beckman Model 126 dual pump and 166 single channel detector on a Vydac C-18 reverse phase column. ^{19}F-NMR spectra were recorded on a Bruker AM-500 (tuned down to 470.56 MHz for fluorine detection) instrument in $CDCl_3$ and referenced externally to $CFCl_3$. Mass spectra were obtained with a cesium ion fast atom bombardment spectrometer. Electrochemistry was performed under Ar in a three-compartment cell consisting of a highly polished glassy carbon working electrode, a Ag/AgCl reference electrode in 1M KCl, and a platinum auxiliary electrode. The working electrode and reference electrode were connected by a modified Luggin capillary. A 1000 W tungsten lamp was used for photolysis experiments.

Crystal Structure Analysis. Deep red crystals of $RuTFPPCl_8$-$(CO)(H_2O)$ were grown by slow evaporation from an ethyl

(39) Brown, G. M.; Hopf, F. R.; Ferguson, J. A.; Meyer, T. J.; Whitten, D. G. *J. Am. Chem. Soc.* **1973**, *95*, 5939−5942.
(40) Tsutsui, M.; Ostfeld, D.; Hoffman, L. M. *J. Am. Chem. Soc.* **1971**, *93*, 1820−1823.
(41) Chow, B. C.; Cohen, I. A. *Bioinorg. Chem.* **1971**, *1*, 57−63.

acetate/hexane solution. A suitable crystal was mounted in a capillary with silicone grease and centered on a CAD-4 diffractometer using Mo Kα radiation. Atomic scattering factors and values for $\Delta f'$ were taken from Cromer and Waber[42] and Cromer;[43] CRYM,[44] MULTAN,[45] and ORTEP[46] computer programs were used. The weights were taken as $1/\sigma^2(F_o^2)$; variances ($\sigma^2(F_o^2)$) were derived from counting statistics plus an additional term, $0.014I^2$; variances of the merged data were obtained by propagation of error plus another additional term, $(0.014\bar{I})^2$.

Ruthenium atom coordinates were obtained from a Patterson map, and the remaining atoms were located with structure factor Fourier calculations. Hydrogen atoms on the solvent molecules were positioned by calculation in idealized locations with staggered geometry and a C−H bond length of 0.95 Å. Of the solvent molecules, only one ethyl acetate site is fully populated (C71, C72, O2, O3, C73, and C74). The second (C81, C82, O4, O5, C83, and C84) is half-populated, near a center of symmetry. The region occupied by hexane is not easily interpreted. There are five peaks in a difference map in an area of broadly diffuse electron density. These five were coplanar within 0.15 Å, so we fitted idealized hexane molecules to the difference density in this plane. Our model has three orientations of the hexane; there may be twice that many. We kept the positional and thermal parameters of these idealized molecules fixed but refined their population parameters independently. The sum of the three was 0.84; we believe this represents some loss of hexane from the crystal during data collection. We kept the populations fixed in the final refinement. The final difference map has peaks of 0.88, 0.82, and 0.79 $Å^{-3}$ and valleys of −1.24 and −0.84 $Å^{-3}$ in this region.

Acknowledgment. We thank Julia Hodge and Toshi Takeuchi for helpful discussions. Assistance with certain experiments was provided by Mike Hill, Sherrie Walsh, and Elaine Marzluff. This work was supported by the NSF, the U.S. Department of Energy, Morgantown Energy Technology Center, the Gas Research Institute, and the Sun Co., Inc. E.R.B. acknowledges the AFOSR and the Parsons Foundation for graduate fellowships.

Supplementary Material Available: Final refined parameters for $RuTFPPCl_8(CO)H_2O$ (Table S1) and the solvent molecule parameters (Table S2), anisotropic displacement parameters (Table S3), complete distances and angles (Table S4), and intermolecular distances less than 3.5 Å (Table S5) (19 pages). Ordering information is given on any current masthead page.

IC940168J

(42) Cromer, D. T.; Waber, J. T. *International Tables for X-ray Crystallography*; Kynoch Press: Birmingham, U.K., 1974; Vol. IV, pp 99−101.
(43) Cromer, D. T. *International Tables for X-ray Crystallography*; Kluwer Academic Publishers: Dordrecht, The Netherlands 1974; Vol. IV, pp 149−151.
(44) Duchamp, D. J. In *Proceedings of the American Crystallographic Association Meeting*, Bozeman, MT, 1964; Paper B14, p 29−30.
(45) Debaerdemaeker, T.; Germain, G.; Main, P.; Refaat, L. S.; Tate, C.; Woolfson, M. M. In MULTAN; Universities of York, England, and Louvain, Belgium, 1988.
(46) Johnson, C. K. In Report ORNL-3794; Oak Ridge National Laboratory: Oak Ridge, TN, 1976.